Photohole Screening Effects in Polythiophenes with Pendant Groups

D.-Q. Feng,[†] A. N. Caruso,[‡] D. L. Schulz,[‡] Ya. B. Losovyj,[§] and P. A. Dowben*,[†]

Department of Physics and Astronomy and the Center for Materials Research and Analysis, University of Nebraska−Lincoln, Lincoln, Nebraska 68588-0111, Center for Nanoscale Science and Engineering, North Dakota State University, Fargo, North Dakota 58102, and Center for Advanced Microstructures and Devices, Louisiana State University, 6980 Jefferson Highway, Baton Rouge, Louisiana 70806

Received: May 23, 2005; In Final Form: July 4, 2005

We compare two mechanisms that dominate the temperature-dependent changes in electronic structure for poly(3-hexylthiophene-2,5 diyl) (P3HT). Structural changes in the relative orientation and configuration of the aromatic ring backbone are observed to occur over a wide range in temperature and affect the local final state screening in photoemission. There are also changes in conductivity and carrier concentration at lower temperatures leading to altered long-range intramolecular screening of photoholes and final state effects that affect excitation spectroscopies including photoemission. For polyethylenedioxythiophene (PEDOT), temperature-dependent changes in the structure and configuration of the polymer backbone are not as significant, although temperature-dependent final state effects are observed.

1. Introduction

Changes in band gap with temperature are often observed with semiconducting polymers[1−6] and can be useful not only as optical temperature indicators but also for thermal recording.[7] Moreover, thermal control of the band gap allows for a continuous variation of electroluminence energies (wavelengths) for polymer light-emitting diodes.[8] Several effects can contribute to thermochromism, and these temperature-dependent effects can be classified into two groups. There are initial state effects as might result from structural changes, or chemical changes that alter the ground-state electronic structure. Final state effects due to changes to electron−phonon coupling, local interactions, carrier concentration, charge mobility, and the correlation energy, although often interrelated, can result in changes to the many electron response (screening) in excitation spectroscopies. These final state effects can affect polaronic hopping, and Coulombic interactions affecting exciton formation, optical excitations, and photoemission.

Experimental and model studies in polythiophenes proposed that thermochromic effects are mainly due to conformational changes instead of electronic interchain interaction.[1−3] Temperature-dependent electronic properties coupled to backbone configuration are observed with other conducting polymers,[4,5,9] poly(3-octyloxy-4-methylthiophene), poly[2-methoxy-5-(2′-ethhexyloxy)-1,4-phenylene-vinylene] and polypyrrole. While the structural distortions contributing to thermochromism may have a profound effect upon conductivity and π-band localization of the highest occupied molecular orbitals of polymers with aromatic backbones,[6,9] the role of defects (gap states) on conductivity is often ignored or overlooked.

In any consideration of defects, it is important to distinguish between two kinds of defects. There are chemical defects such as "missing hydrogen" on an aliphatic pendant group, or some chemical impurity. Such defects are seen to decrease the band gap, as is the case in poly[2-methoxy-5-(2′-ethyl-hexyloxy)-1,4-phenylene-vinylene] (MEH-PPV).[10] There are structural defects that occur, in the absence of any chemical defect, due to disorder in the molecular structure. For example, the mobilities[9] in organic field-effect transistors at elevated temperature were correlated with structural distortions in the poly-(3-hexylthiophene-2,5 diyl) layer of the transistor[1], but the only "defect" considered was disorder in the relative orientation of the adjacent aromatic rings and associated pendant groups.

Poly(3-hexylthiophene-2,5 diyl) (P3HT) was one of the first aromatic polymers found to exhibit thermochromism in terms of thermally induced conjugation defects in the aromatic backbone.[1,2,6] Thermochromism has been inferred from photoemission studies of undoped P3HT, as a function of temperature,[1,2] combined with the optical absorption spectra,[2] and explained on the basis of valence effective Hamiltonian (VEH) quantum chemical calculations,[1,11] without invoking chemical defects.

A very small numbers of chemical defects may contribute significantly to the hopping conductivity so that defect state trapping and hopping conductivity are more significant than the changes in band gap when considering changes in conductivity below room temperature, as has been explored in more detail elsewhere.[6] The dominant role of defects at low temperatures (well below room temperature), in influencing conductivity, does not exclude the possibility that structural distortions influence thermochromism. By comparing a more rigid polythiopehene, polyethylenedioxythiophene (PEDOT), with a far less rigid polythiophene, poly(3-hexylthiophene-2,5 diyl) (P3HT), the origin of the temperature-dependent changes in band gap and conductivity can be explored in some detail. In this regard, we report the results of an investigation of thermochromism in two aromatic backbone semiconducting polymers using light polarization-dependent ultraviolet photoemission spectroscopy, high-resolution ultraviolet photoemission, and inverse photoemission. We compare these results to the calculated changes in the molecular orbital binding energies that accompany the tilting of aromatic rings within the polymer backbones, relative to one another.

* Corresponding author. Phone: (402) 472-9838. Fax: (402) 472-2879. E-mail: pdowben@unl.edu.
[†] University of Nebraska−Lincoln.
[‡] North Dakota State University.
[§] Louisiana State University.

10.1021/jp052712n CCC: $30.25
Published on Web 08/10/2005

2. Experimental and Theoretical Details

A 1 wt % solution of poly(3,4-ethylenedioxythiophene)-block-poly(ethylene glycol) (PEDOT/PEG) in nitromethane (Aedotron P) was procured from Aldrich and sonicated prior to spin coating. Aedotron P is PEDOT/PEG doped with para-toluene as manufactured by TDA Research, Inc. Regioregular poly(3-hexylthiophene-2,5 diyl) (P3HT) was purchased from Aldrich and dissolved in chloroform for spin coating, as employed elsewhere.[1,2,4,9−12] Combined high-resolution ultraviolet photoemission and inverse photoemission were undertaken to study the molecular orbital placement of both occupied and unoccupied orbitals of the polymer films. In both types of photoemission measurements, as well as in the inverse photoemission studies, the binding energies are referenced with respect to the Fermi edge of gold or tantalum, measured at 80 K, in intimate contact with the sample surface. In photoemission, all photoelectrons were collected normal to the substrate surface, while in inverse photoemission, the electrons were incident normal to the surface, that is, $k = 0$ or $\bar{\Gamma}$, to preserve the highest possible local point group symmetry.

The high-resolution ultraviolet photoemission spectra (UPS) were taken using a helium lamp at $h\nu = 21.2$ eV (He I) and a Scienta 200 hemispherical electron analyzer at the Center for Advanced Microstructures and Devices synchrotron radiation facility in Baton Rouge, LA (CAMD). The combined resolution in our high-resolution ultraviolet photoemission experiments was better than 10 meV, as inferred from widths of the Ar $3p_{1/2}$ (15.9 eV) and $3p_{3/2}$ (15.7 eV) lines in photoionization spectra, as described in detail elsewhere.[13]

The light polarization-dependent ultraviolet photoemission spectroscopies were carried out using synchrotron light, dispersed by a 3 m toroidal grating monochromator, at CAMD, as described in detail elsewhere.[4,10,14] The measurements were performed under ultrahigh vacuum conditions (3×10^{-10} Torr) employing a hemispherical electron energy analyzer with an angular acceptance of $\pm 1°$.

For the angle-resolved measurements, the combined resolution of the electron energy analyzer and monochromator varied between 0.10 and 0.25 eV. All angles (both light incidence angles as well as photoelectron emission angles) reported herein are with respect to the substrate surface normal. Because of the highly plane polarized nature of the dispersed synchrotron light through the toroidal grating monochromator, the large light incidence angles result in a vector potential **A** more parallel to the surface normal (p-polarized light), while smaller light incidence angles result in the vector potential **A** residing more in the plane of the surface (s-polarized light) in the geometry of our experiment. The polarization dependence can be related to the photoemission selection rules resulting in changes in the cross-section of symmetry specific molecular orbitals. The details of selection rule formalism are laid out elsewhere,[15,16] and, as is typical with large organic molecules,[4,6,10,15] the partial cross-section for photoemission varies according to the orientation of the light vector potential **A** of the incident plane polarized light and the symmetry of the initial state ψ_i, assuming that the final state wave function ψ_f (for electrons collected along the surface normal) is fully symmetric, according to:

$$\left(\frac{d\sigma}{d\Omega}\right)_{PES} \propto |\langle\Psi_f|A\cdot p + p\cdot A|\Psi_i\rangle|^2 \delta(E_f - E_i - h\nu) \quad (1)$$

where $\mathbf{A}\cdot\mathbf{p}$ is the effective dipole operator.

The inverse photoemission spectra were obtained by using variable incident energy electrons with a fixed energy UV detector (a Geiger−Müller detector). The instrumental line width is ∼400 meV, as described elsewhere.[17,18] All inverse photoemission spectra (IPES) were obtained with the electron gun at normal incidence and the detector positioned at 45° off the surface normal.

Theoretical calculations of the electronic structure of regioregular poly(3-hexylthiophene-2,5 diyl) (P3HT) and polyethylenedioxythiophene (PEDOT) were undertaken by PM3-NDO (neglect of differential overlap) with the HyperChem package.[19,20] Similar semiempirical molecular orbitals calculations have recovered much of the detail observed in large molecular systems using photoemission and inverse photoemission, including reproducing, with reasonable agreement, the highest occupied molecular orbital (HOMO) to lowest unoccupied molecular orbital (LUMO) gap for *closo*-carborane molecular films,[21] fluorinated polymer films,[22] multilayer films of biphenyldiisocyanide,[23] biphenyldimethyldithiol,[24] and tris(8-hydroxyquinoline) aluminum (Alq_3).[25] Hydrogen terminated (to prevent excessive folding) short chain length (from 1 to 16 repeat units for P3HT and 1 unit for PEDOT) polymers were used for our simplistic model calculations, as has been done elsewhere.[6,10] Because $\pi-\pi$ interchain stacking is believed to play an important role in determining the band gap and the film conductivity,[26−28] calculations were undertaken for both a single chain and double chains (π-packed) of regioregular poly(3-hexylthiophene-2,5 diyl) (P3HT), again as undertaken elsewhere.[6,10] Geometry optimization of the system was performed obtaining lowest unrestricted Hartree−Fock (UHF) energy states.

A calculated density of states (DOS) was obtained by applying equal Gaussian envelopes of 1 eV full width half-maximum to each molecular orbital (to account for the solid state broadening in photoemission) and then summing. This calculated density of states, together with a rigid energy shift of 5.3 eV applied to the calculated electronic structure, is compared to the photoemission. The model calculations of the density of states do not account for photoemission and inverse photoemission matrix element effects, so that the comparison to ultraviolet photoemission must be considered only qualitative.

3. Evidence for Dielectric Character of P3HT

Overall, there is good agreement between experiment and the expected ground-states molecular orbital binding energies obtained from our calculations. We can assign the various photoemission and inverse photoemission features, as shown in Figure 1, by comparing the occupied molecular orbitals derived from semiempirical ground-state calculations, as is typical with large molecular systems.[4,10,15,21−25] The difference between orbital energies (Figure 2), obtained in theory and referenced to the vacuum level, and the experimental binding energies with respect to the Fermi level, obtained for regioregular poly(3-hexylthiophene) from the photoemission spectra, is about 5.3 eV, as was observed in comparing the calculated spectra with other conducting polymers.[10] This shift between theory and experiment is similar to that observed for *closo*-carborane molecular films,[21] fluorinated polymer films,[22] multilayer films of biphenyldiisocyanide,[23] biphenyldimethyldithiol,[24] poly[2-methoxy-5-(2′-ethyl-hexyloxy)-1,4-phenylene-vinylene] (MEH-PPV),[10] and like molecules.[15]

As seen from Figure 2, many features, from the photoemission and inverse photoemission spectra (Figure 1), can be assigned to groups of molecular orbitals such as the features at −3.8 eV (a), −7.5 eV (b), −10.2 eV (c), and −11.3 eV (d), but father away from the Fermi level the calculation underestimates the

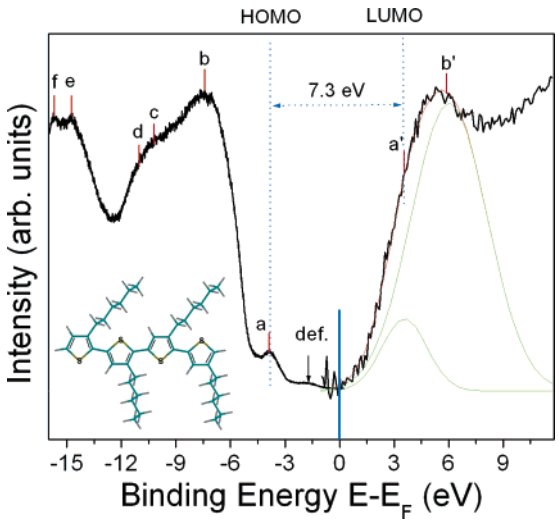

Figure 1. Occupied (left) and unoccupied (right) molecular orbital contributions of regioregular P3HT to the photoemission and inverse photoemission, respectively. The experimental molecular HOMO−LUMO gap is 7.3 eV for P3HT. Many features from photoemission spectrum are labeled for identification: (a) 3.8 eV, (b) 7.5 eV, (c) 10.2 eV, (d) 11.3 eV, (e) 14.7 eV, (f) 15.7 eV, (a′) 3.5 eV, and (b′) 6.0 eV. The photoemission spectrum was taken with unpolarized He I (21.2 eV), with the photoelectrons collected normal to the surface, and inverse photoemission spectrum was taken at normal incidence. The inset shows a schematic of a single chain of regioregular P3HT.

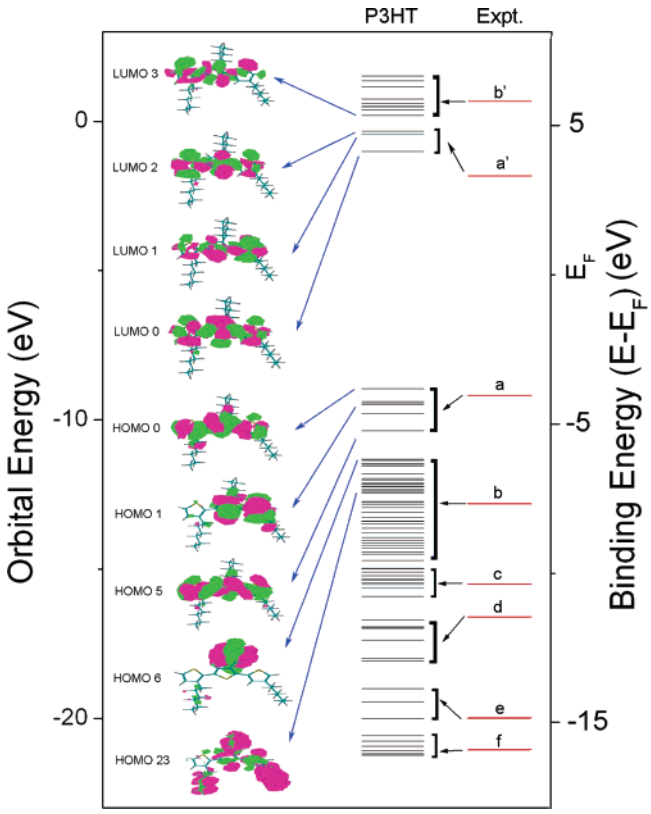

Figure 2. The geometry optimization calculated ground-state molecular orbital energies of three monomers of regioregular P3HT as compared to experimental binding energies with respect to the Fermi level. This includes a few unoccupied molecular orbitals down to the lowest unoccupied molecular orbital, as well as the occupied molecular orbitals referenced to the vacuum level. Selected molecular orbitals (HOMO) are shown left. The ground-state free molecular HOMO−LUMO gap of 7.7 eV was derived for a short single chain P3HT and is intended to be representative (not quantitative) only for the purposes of visualizing the molecular orbital level ordering.

binding energy as is the case of the photoemission features at −14.7 eV (e), −15.7 eV (f) and the inverse photoemission features at 3.5 eV(a′) and 6.0 eV (b′). This is a standard problem with these types of molecular orbital calculations, not to mention the flaws in comparing ground-state calculations to the results obtained from final state spectroscopies.

The very weak photoemission feature at −1.7 eV binding energy (denoted as "def." in Figure 1) cannot be assigned to any corresponding molecular orbital in our molecular orbital calculations. We assign this feature of −1.7 eV to a defect state, which could be a consequence of impurities and/or "chemical" defects, although this feature has been ascribed to band structure effects accompanying the ordering of the aromatic chain backbone.[1] The nature of the "defects" that lead to this state cannot be uniquely identified from our data, although there are several possibilities. As seen in Figure 3, limited loss of regioregularity (Figure 3a), an oxygen bridging two pendant groups (Figure 3b), selected dehydrogenation resulting in a pendant group linking two adjacent thiophenes (Figure 3c), and loss of $\pi-\pi$ stacking either through tilting of adjacent polymer chains (Figure 3d) or as a result of a lateral displacement of adjacent polymer chains (Figure 3e) could well result in the appearance of defects states within the HOMO−LUMO gap of regioregular poly(3-hexylthiophene-2,5 diyl) (P3HT). Two photon ionization experiments suggest the presence of polaronic gap states or defects states just below the conduction band edge, pinned above the Fermi level,[29] which suggests the loss of regioregularity on the basis of our model calculations. Such defect states would appear in the optical absorption of regioregular poly(3-hexylthiophene-2,5 diyl) (P3HT) in solution as well as explain the tailing density of states in the inverse photoemission spectra from the conduction band edge to the just above the Fermi level, as seen in Figure 1. We note that the binding energy of the defect states at 1.7 eV is close to a strong absorption band, at 1.8 eV, that has been attributed to injected carriers and assigned to polarons.[3,30,31]

From the combined photoemission and inverse photoemission spectra as shown in Figure 1, we see that the chemical potential of P3HT (the Fermi level) is placed within the highest occupied molecular orbital (HOMO) and lowest molecular orbital (LUMO) gap, with the Fermi level slightly closer to the LUMO, similar to the band offset description for undoped P3HT in refs 6 and 32. The experimental molecular HOMO−LUMO gap is 7.3 ± 0.2 eV for P3HT, which is consistent with the 6.4 eV gap estimated from the gas-phase X-ray photoelectron spectroscopy on the P3HT[33] monomer. As a consequence of the placement of the highest occupied and lowest unoccupied molecular orbitals, relative to the Fermi level, P3HT is not very p-type, and the electronic structure in the vicinity of the Fermi level is more characteristic of an n-type insulator, given the position of the chemical potential (Fermi level).

To correctly estimate the HOMO−LUMO gap, the better calculations would be undertaken on a paracrystalline polymer slab. Although not ideal, we have estimated the HOMO−LUMO gap based on calculations undertaken on increasingly longer single and double (two parallel) chain lengths, as summarized in Figure 4. It is clear that the calculated HOMO−LUMO gap does decrease by increasing the number of monomers and chains. The influence of the $\pi-\pi$ interchain stacking (schematically shown as the inset to Figure 4) on the HOMO−LUMO gap for double (two parallel) chains of P3HT appears to be less significant than chain length. The HOMO−LUMO gap for the calculation shown in Figure 2 is only slightly larger than the

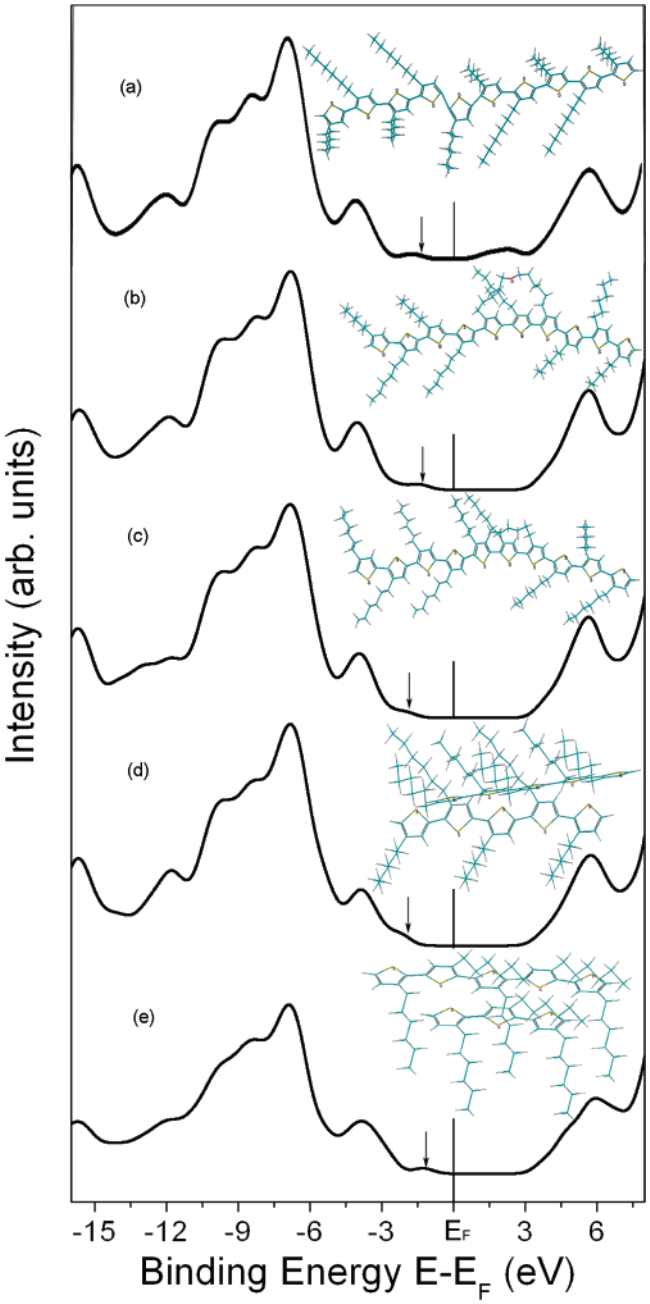

Figure 3. The calculated density of states (DOS) for several types of structural defects as might occur for a 10-monomers chain length regioregular P3HT. These structural and chemical defects include the limited loss of regioregularity (a), an oxygen bridging two pendant groups (b), selected dehydrogenation resulting in a pendant group linking two adjacent thiophenes (c), and loss of $\pi-\pi$ stacking either through tilting of adjacent polymer chains (d) or as a result of a lateral displacement of adjacent polymer chains (e), but is by no means a complete nor exhaustive representative of possible defects that may occur in regioregular P3HT thin films. The corresponding geometries of P3HT are shown in the inset above each DOS.

value calculated for longer double chains of P3HT. Increasing chain length does result in a decrease in the calculated HOMO−LUMO gap, but this is mostly significant for chain lengths shorter than 5 monomers (Figure 4).

The value of 6.9 eV for the HOMO−LUMO gap was abstracted for the longer double chains of P3HT, as shown in Figure 4. The theoretical estimate of the HOMO−LUMO gap of 6.9 eV is in good agreement with our value from experiment (7.3 ± 0.2 eV). In general, comparison of the experimental

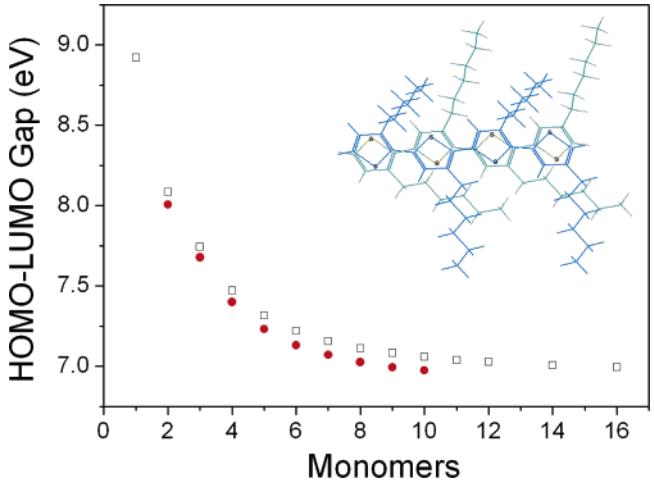

Figure 4. The HOMO−LUMO gap abstracted from the calculated ground-state molecular orbital of energies of regioregular P3HT for an increasing number of monomers (repeat units) of P3HT. A single chain (□) is compared to a double chain (red ●) of P3HT. Shown in the inset is the double chain structure of the regioregular P3HT.

results with theory excludes the assignment of the weak photoemission feature at 1.7 eV below the Fermi level to a molecular orbital characteristic of regioregular P3HT, as noted elsewhere.[6]

Even taking into account the photoemission feature at small binding energies, at all temperatures investigated the highest occupied molecular orbital (HOMO) to lowest unoccupied molecular orbital (LUMO) gap still remains very large (e.g., at 300 K, a gap of about 5.3 eV was found). This 5.3 eV gap cannot be reconciled with the molecular orbital calculations of regioregular P3HT in the absence of any structural defects or chain-to-chain packing "problems" and is indicative of defect states as discussed above.

We are forced to conclude that undoped, poly(3-hexylthiophene-2,5 diyl) is an insulator. As a result, small changes in band gap should have little effect on conductivity, given the very large highest occupied to lowest unoccupied (HOMO−LUMO) gaps, even when structural defects are present. Thermochromic effects are still possible as extramolecular $\pi-\pi$ interactions can be altered with structural changes (as indicated in Figure 3), thus affecting the effective local band gap as well as the local screening, by altering the charge trapping and changing the carrier mobilities. The $\pi-\pi$ interactions and associated effects on carrier concentrations and carrier mobility can also significantly affect the more long-range intramolecular screening.

In the absence of structural and chemical defects, the experimental and calculated HOMO−LUMO gaps here are very different from the values observed in optical spectroscopy for P3HT (about 2.1−2.5 eV[3,9,26,27,30,34]). Even taking into account the fact that Coulombic intramolecular interaction effects occur with optical excitations, this value is much smaller than the HOMO−LUMO gap obtained in our combined photoemission and inverse photoemission studies as well as in the ground-state molecular orbital calculations. This large difference between combined photoemission and inverse photoemissions studies and optical absorption can only be due to defects, impurities, or extrinsic carriers, with possible polaronic contributions. The inconsistencies between the combined photoemission results and the optical absorption data, seen here in regioregular poly(3-hexylthiophene-2,5 diyl), are similar to the example of poly[2-methoxy-5-(2′-ethyl-hexyloxy)-1,4-phenylene-

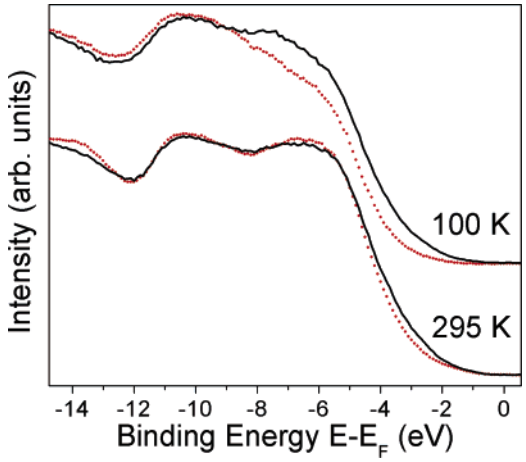

Figure 5. Comparison of the light polarization photoemission spectra of regioregular P3HT taken with p polarized light (red ●) and s+p polarized light (−) for temperatures of 100 and 295 K separately. The spectra were taken at a photon energy of 32 eV, and the photoelectrons were collected at normal emission.

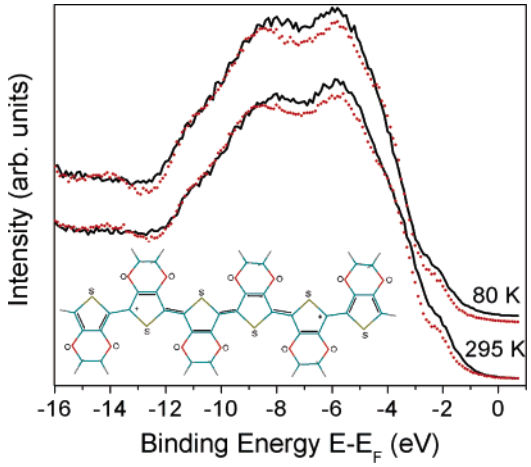

Figure 6. Comparison of the light polarization photoemission spectra of PEDOT taken with (red ●) p polarized light and (−) s+p polarized light for temperatures of 80 and 295 K separately. The spectra were taken at a photon energy of 40 eV, and the photoelectrons were collected at normal emission. The inset shows a schematic of a single unit of PEDOT.

vinylene] (MEH-PPV)[10] where optical absorption also suggests a far smaller HOMO−LUMO gap and is indicated by photoemission.

4. Structural Changes in the P3HT and PEDOT Aromatic Chain Backbone

Consistent with previous studies,[1,2] we see strong temperature-dependent light-polarization effects in the photoemission spectra of P3HT, as shown in Figure 5. The changes in the photoemission spectra obtained by changing the light incidence angle from a large incidence angle of 70° (p polarized light) to a smaller incidence angle of 43° (s+p polarized light) is far more significant at 100 K than at 295 K. The differences in the light polarization photoemission largely disappear by room temperature (Figure 5). On the basis of these results, we can conclude that regioregular poly(3-hexylthiophene-2,5 diyl) (P3HT) is far more highly ordered at low temperatures than at higher temperatures. Indeed, to obtain these photoemission results, this ordering requires that the aromatic thiophene rings are coplanar at lower temperatures.

The evidence of strong light polarization effects suggests a strong preferential orientation of the polymer chains as has been observed in other polymer systems.[4,10,15] Unfortunately, due to the low symmetry of P3HT and PEDOT combined with the large number of overlapping molecular orbitals that contribute to each photoemission feature, we cannot conclusively ascertain, from Figures 5 and 6, the preferential orientation adopted by P3HT and PEDOT in our films, but an orientation similar to that proposed in ref 12, with the molecular chain parallel to the plane of the film and the aromatic ring of the backbone perpendicular to the film plane, seems likely for P3HT.[12] Temperature-independent polymer chain orientational defects, such as those illustrated in Figure 3d, are largely excluded by the light polarization photoemission.

The strong evidence of increasing order, along the aromatic chain backbone with decreasing temperature for P3HT, is consistent with the model proposed by Salaneck and co-workers,[1] who infer from their data that with increasing temperature there occurs a rotation of increasingly smaller segments (segments with smaller numbers of aromatic rings) with respect to the adjacent segments. On the basis of the photoemission results, Salaneck and co-workers[1,2] proposed that the thiophene rings are coplanar at low temperatures and the torsion angle or disorder along the aromatic backbone increases with increasing temperature, and these structure changes occur near or above room temperature.[1−3] From the light polarization-dependent photoemission, we infer that changes in the regioregular P3HT polymer backbone geometry occur well below room temperature for P3HT, and the structure changes are gradual. Other conducting polymers exhibit changes in the orientation of the aromatic rings in the polymer backbone with temperature similar to those reported here for P3HT, including polypyrrole,[4] so P3HT is not unusual in this regard.

The geometry optimized structure for P3HT does result in a greater twist in the backbone conformation, which is consistent with the light polarization-dependent photoemission data at higher temperatures. The $\pi-\pi$ interactions are expected to suppress torsion at lower temperatures when the phonon contributions that weaken intermolecular interactions are suppressed.

Such temperature-dependent changes in the orientational (dis)-order of the backbone structure have not been observed for PEDOT, as seen from angle resolved polarization-dependent photoemission spectra (Figure 6). While there are significant temperature-dependent changes of the valence band photoemission binding energies between 295 and 80 K, as seen from Figure 7, few of these changes are associated with changes in the polymer backbone structure as would be manifest in light polarization-dependent photoemission (Figure 6). The indications of preferential bonding orientation for PEDOT, from the light polarization-dependent photoemission (Figure 6), do not seem to be very temperature sensitive. The enhancement of the different photoemission features for each light polarization (p polarized versus s+p polarized light) is about the same for 295 and 80 K.

The strong dipole interactions and rigidity imparted to the thiophene backbone by the ethylenedioxy group may suppress thermochromic effects in PEDOT consistent with our molecular orbital calculations. Whatever the cause, PEDOT can be interpreted as a planar rigid rod over a wide range in temperature. Unlike the case for P3HT, only small structural changes for PEDOT were observed in geometry optimized calculations, again consistent with the experimental data. The model calcula-

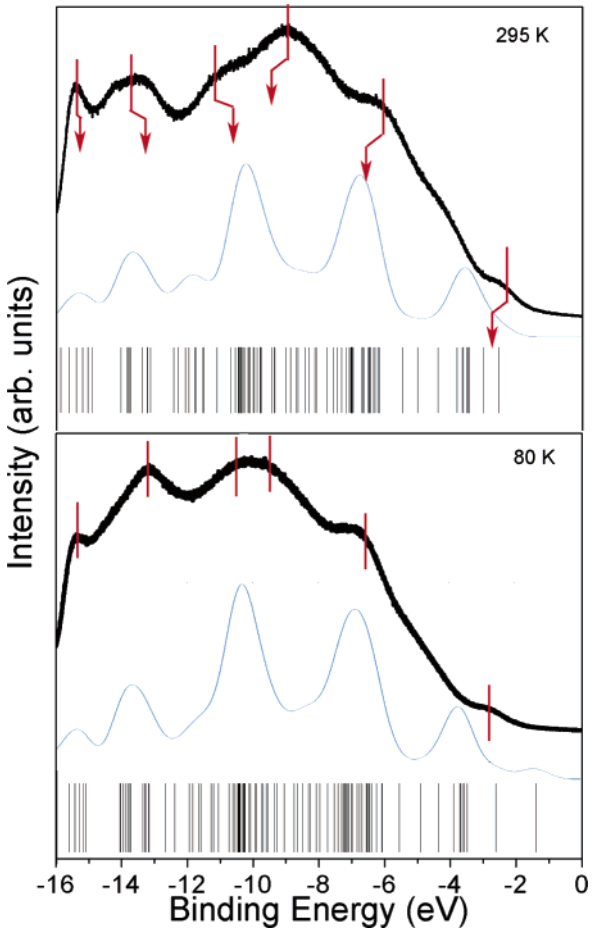

Figure 7. Occupied molecular orbital contributions of PEDOT to the photoemission spectra (taken at 295 K (top) and 80 K (bottom)) are compared to the calculated ground-state molecular orbital energies for 1 unit of a single chain. The calculated upper DOS curve (295 K) comes from an optimized twisted geometry for PEDOT, and the lower one (95 K) comes from coplanar geometry. Bars indicate the calculated orbital energies of the molecular orbitals, together with a calculated density of states that assumes all molecular orbitals contribute equally to the experimental density of states. The experimental shifts in the photoemission featuring binding energies, with temperature, have been drawn in red to guide eye. The photoemission spectrum was taken with unpolarized He I (21.4 eV), with the photoelectrons collected normal to the surface.

tions indicate that significant ring reorientation from one aromatic ring to the next is energetically very "expensive" and therefore very unlikely. Although not part of the planar backbone structure for the PEDOT, the geometry optimized calculation shows the twist angle between oxygen atoms increases very little with increasing temperature. The charge (molecular orbital density) is localized on the aromatic ring due to the close proximity of the oxygen atoms, resulting in ring components that are much more rigid for PEDOT than for P3HT.

The loss of coplanar aromatic ring structure in the polymer backbone leads to changes in the HOMO−LUMO gap, and some thermochromism for both PEDOT and P3HT, even for the small structural distortions predicted by theory for PEDOT. This is summarized in Figure 7 (PEDOT) and Figure 8 (P3HT). Unfortunately, tilting of the aromatic rings with respect to one another with increasing temperature does not fully account for the temperature-dependent effects in the occupied molecular orbital structure observed in photoemission for PEDOT (Figures 6 and 7) and P3HT (Figure 9).

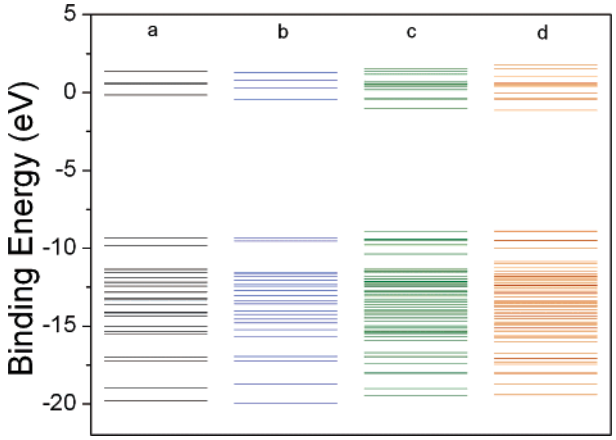

Figure 8. Theoretical calculations of the lowest unoccupied molecular orbital (LUMO) and highest occupied molecular orbital (HOMO) energy state for regioregular P3HT. The calculations for one monomer (a, b) and three monomers (c, d) predict a larger HOMO−LUMO gap for the twist (a, c) geometry structure than for the "flat" (b, d) orientation of the aromatic rings in P3HT, with 9.23 eV for 1 monomer and 7.94 eV for 3 monomers in a twist geometry, as opposed to 8.92 eV for 1 monomer and 7.74 eV for 3 monomers in a flat geometry.

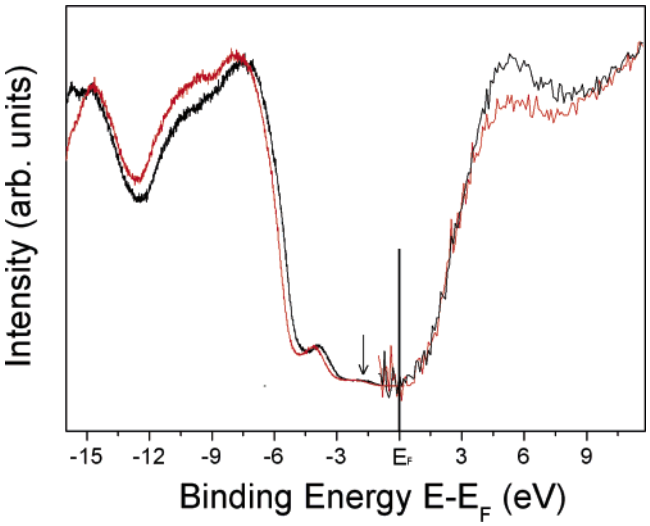

Figure 9. The changes in the combined photoemission (left) and inverse (right) photoemission spectra of regioregular P3HT as a function of temperature. Spectra are shown for 295 K (black) and 215 K (red). The photoemission spectrum was taken with unpolarized He I (21.4 eV), with the photoelectrons collected normal to the surface, and the inverse photoemission spectrum was taken at normal incidence.

5. Structural Changes versus State-Dependent Screening Effects in Temperature

Thermochromism, particularly in photoemission and excitation spectroscopy, need not be restricted to changes in the initial (ground-state) electronic structure, as noted in the Introduction. Changes in photohole screening,[35] electron phonon coupling,[13] and other effects can result in profound photoemission and absorption final state effects. Among the problems of interpreting thermochromic behavior are that the thermally induced transition is the gradual change from a planar rigid rod backbone conformation of coplanar aromatic rings at lower temperatures to a more random twisting conformation at higher temperatures. The charge localization due to temperature-dependent trapping and mobility, as a result of chemical defects, is also gradual if the chemical defects are heterogeneous. If losses in conductivity are attributable to defects of a particular type, then temperature

dependence and state selective screening in the photoemission processes may provide some insight into the origin.

Photoemission and inverse photoemission measurements were used to confirm the decrease in screening (of the photohole) and an increase in the insulating character of the P3HT and PEDOT films with decreasing temperature. The significant increase of the valence band edge binding energy is not accompanied by significant changes in the unoccupied states (Figure 9) for P3HT. Such changes, as do occur in relative photoemission and inverse photoemission peak intensities for P3HT (Figure 9), can be attributed to the changes in the polymer geometry (i.e., twisting) that occurs with temperature, but the changes in binding energies are difficult to reconcile with ground-state calculations. This implicates final state effects as contributing to the observed shifts in binding energies.

The binding energies resulting from the occupied molecular orbitals for P3HT (Figure 9) and PEDOT (Figure 7) are generally observed to increase (binding energies in absolute value, i.e., move away from the chemical potential) with decreasing temperature. The exceptions are the photoemission features at greater binding energies (binding energies greater than −10 eV, or farther from the chemical potential than 10 eV), which actually increase in binding energy (or move away from the chemical potential) with decreasing temperature.

As temperature decreases, the three pronounced photoemission features closest to the chemical potential move away from Fermi edge (toward higher binding energies), indicating formation of a more insulating phase with decreasing temperature for both P3HT (Figure 9) and PEDOT (Figure 7). These increases in binding energy can only be explained by a general decrease in screening of the photoemission final state[35] due to electron and hole localization, a loss of carrier conductivity, and a decrease of carriers (increased carrier trapping). By comparing the changes in photoemission to the significant changes in bulk conductivity in the region of 200 K, it is clear that electron and hole localization, a loss of carrier conductivity, and a decrease of carriers (increased carrier trapping) in P3HT does have a pronounced effect on the photoemission binding energies.[6]

Those photoemission features father away from the chemical potential, as noted above, move toward the Fermi level with decreasing temperature for P3HT (Figure 9). The decrease in binding energy with decreasing temperature in these bands is consistent with the increase in final state screening of more shallow core like carbon 2s and sulfur 3s weighted molecular orbitals and a decrease in binding energy that is expected to accompany the more coplanar aromatic ring geometry. The increase in final state screening with decreasing temperature for these more core like molecular orbital photoemission features will be due to the $\pi-\pi$ intermolecular interactions that lead to stronger intermolecular photoemission screening.[35]

For PEDOT, the photoemission features father away from the chemical potential, as noted above, also move toward the Fermi level with decreasing temperature (Figure 7). Because the ethylenedioxy pendant groups suppress "twisting", the decrease in binding energy with decreasing temperature in these bands cannot as easily be attributed to an increase in final state screening of more shallow core like carbon 2s and sulfur 3s weighted molecular orbitals due to an increase in $\pi-\pi$ intermolecular interactions that is expected to accompany the more coplanar aromatic ring geometry. Rather, the decrease in binding energy due to $\pi-\pi$ intermolecular interactions must be influenced by phonon interactions as well as the polymer backbone ring geometry. The $\pi-\pi$ intermolecular interactions must be strongly enhanced as the phonon modes are quenched with decreasing temperature.

In fact, theory predicts generally larger photoemission binding energies and a larger HOMO−LUMO gap for a twisted geometry than a flat geometry by more than 300−400 meV for even just a very short single chain of P3HT as well. As shown in Figure 8, twisting the P3HT backbone (i.e., tilting the aromatic ring in the polymer backbone with respect to one another) increases the HOMO−LUMO band gap, although in our molecular orbital calculations for short chain polymer lengths (both 1 and 3 monomers), the change in the HOMO−LUMO gap is quite small between "twisted" and coplanar geometry. We find a larger gap observed for the "twisted" configuration as compared to the coplanar configuration, neglecting strong interchain interactions.

Neglecting the photoemission screening effects, the role of $\pi-\pi$ stacking is generally ambiguous at present. In the condensed solid film, this is effect expected to be even greater for π stacked polymer chain lengths, if the effective HOMO−LUMO gap is dominated by $\pi-\pi$ interactions. In part, this very different expectation from theory is even more difficult to reconcile with the experimental results when one considered that $\pi-\pi$ intermolecular interactions are suppressed with the loss of the coplanar aromatic ring geometry that occurs with increasing temperature. This loss of $\pi-\pi$ intermolecular interactions should lead to even bigger increases in band gap and weaker intermolecular photoemission screening, which is generally not observed in the photoemission. Defects in the relative chain stacking, also as a result of the loss of $\pi-\pi$ interactions, could result in a decrease in the HOMO−LUMO gap, as indicated by Figure 3d and e.

While the temperature dependent photoemission binding energy shifts P3HT and PEDOT share many similarities, direct comparison is complicated not only by the different pendant groups. The para-toluenesulfonate, like perchlorate dopants, will tend to dope the PEDOT *n*-type. Our PDOT films do not appear to be strongly *p*-type, judging from the photoemission spectra in Figure 7, but the presence of dopants complicates any assignment of the molecular orbital specific screening, in the photoemission of PEDOT.

6. Summary

For both PEDOT and P3HT, we suggest that the dominant contributions to thermochromic effects occur from electron and hole localization, a loss of carrier conductivity, and a decrease of carriers (increased carrier trapping). These changes in the photohole screening result in profound final state effects in photoemission. We suggest that $\pi-\pi$ interactions, state selective screening effects of the photoemission photohole, and other condensed matter effects lead to photoemission screening effects that are very much like state selective sample charging. We do not exclude changes in the initial state from contributing to thermochromic effects, but initial or ground-state changes in electronic structure cannot be the origin of all thermochromic effects.

The phonon contributions to the structural changes in thermochromic P3HT and PEDOT are very different. There is a strong correlation between the electronic structure and backbone conformation of P3HT. For P3HT, the backbone configuration affects the $\pi-\pi$ intermolecular interactions, but for PEDOT, $\pi-\pi$ intermolecular interactions become weaker with increasing temperature without major changes in backbone conformation that are evident in angle-resolved photoemission. Indeed, the change in backbone structure for PEDOT is quite

small; thus we associate some thermochromic effects in PEDOT to the strong phonon electron coupling intermolecular structural distortions related to phonons.

We cannot identify the exact nature of the polymer chain packing defects and the intramolecular defects that may occur, and do occur, from the data presented here. The further investigation of the influence of well-characterized defect states as well as different interchain stacking arrangements is clearly indicated. In addition, comparison of not only photoemission and inverse photoemission, but also photoabsorption and photoexcitation spectroscopies with solid-state calculations of various conducting polymers, is indicated. Such solid-state calculations should, of necessity, include both band structure effects and on-site correlation energies for the undoped polymer systems. Like the inorganic semiconductors, organic semiconductors may prove to exhibit many correlation effects, even if there are no band bending effects as observed in the more conventional inorganic semiconductors.

Acknowledgment. This work was supported by the National Science Foundation through grant CHE-0415421 and the NSF "QSPINS" MRSEC (DMR-0213808), the Defense Microelectronics Activity (DMEA) under agreement CMEA90-02-2-0218, and the NSF through ND EPSCoR grant EPS-0447679. We wish to thank the Center for Advanced Microstructures and Devices, which is funded by the State of Louisiana, and S. Balaz, L.G. Rosa, and B. Doudin for their technical assistance. We would like to acknowledge some very helpful discussions with T. Stuckless.

References and Notes

(1) Salaneck, W. R.; Inganäs, O.; Themans, B.; Nilsson, J. O.; Sjögren, B.; Österholm, J.-E.; Bredas, J. L.; Svensson. S. *J. Chem. Phys.* **1988**, *89*, 4613.

(2) Inganäs, O.; Salaneck, W. R.; Österholm, J.-E.; Laakso, J. *Synth. Met.* **1988**, *22*, 395. Salaneck, W. R.; Inganäs, O.; Nilsson, J. O.; Österholm, J.-E.; Themans, B.; Bredas, J. L. *Synth. Met.* **1989**, *28*, C451. Inganäs, O.; Gustafsson, G.; Salaneck, W. R.; Österholm, J.-E.; Laakso, J. *Synth. Met.* **1989**, *28*, C377. Zerbi, G.; Chicrichetti, B.; Inganäs, O. *J. Chem. Phys.* **1991**, *94*, 4646. Eklebad, P. O.; Inganäs, O. *Polym. Commun.* **1991**, *32*, 436.

(3) Tachibana, H.; Hosaka, N.; Tokura, Y. *Macromolecules* **2001**, *34*, 1823. Leclerc, M.; Faïd, K. *Adv. Mater*. **1997**, *9*, 1087. Rughooputh, S. D. D. V. *Synth. Met.* **1996**, *80*, 195. Yoshino, K.; Nakajima, S.; Onoda, M.; Sugimoto, R. *Synth. Met.* **1989**, *28*, C377. Winokur, M. J.; Spiegel, D.; Kim, Y.; Hotta, S.; Heeger, A. J. *Synth. Met.* **1989**, *28*, C419. Tashiro, K.; Ono, K.; Minagawa, Y.; Kobayashi, M.; Kawai, T.; Yoshino, K. *J. Polym. Sci., Polym. Phys. Ed*. **1991**, *29*, 1223. Garreau, S.; Leclerc, M.; Errien, N.; Louarn, G. *Macomolecules* **2003**, *36*, 692. DiCésare, N.; Belletête, M.; Marrano, C.; Leclerc, M.; Durocher, G. *J. Phys. Chem. A* **1999**, *103*, 795. DiCésare, N.; Belletête, M.; Leclerc, M.; Durocher, G. *J. Phys. Chem. A* **1999**, *103*, 803. DiCésare, N.; Belletête, M.; Garcia, E. R.; Leclerc, M.; Durocher, G. *J. Phys. Chem. A* **1999**, *103*, 3864. Roux, C.; Bergeron, J. Y.; Leclerc, M. *Makromol. Chem.* **1993**, *194*, 869. DiCésare, N.; Belletête, M.; Durocher, G.; Leclerc, M. *Chem. Phys. Lett*. **1997**, *275*, 533.

(4) Choi, J.; Chipara, M.; Xu, B.; Yang, C. S.; Doudin, B.; Dowben, P. A. *Chem. Phys. Lett.* **2001**, *343*, 193.

(5) Roux, C.; Leclerc, M. *Macromolecules* **1992**, *25*, 2141. Kim, Y. H.; Spiegel, D.; Hotta, S.; Heeger, A. J. *Phys. Rev. B* **1988**, *38*, 5490.

(6) Caruso, A. N.; Feng, D.-Q.; Losovyj, Y. B.; Shulz, D.; Balaz, S.; Rosa, L. G.; Sokolov, A.; Doudin, B.; Dowben, P. A., submitted.

(7) Hirola, N.; Hisamatsu, N.; Maeda, S.; Tsukahara, H.; Hyodo, K. *Synth. Met.* **1996**, *80*, 67.

(8) Berggren, M.; Gustafsson, G.; Ingans, O.; Anderson, M. R.; Wennerstrom, O.; Hjerlberg, T. *Appl. Phys. Lett.* **1994**, *65*, 1489.

(9) Zen, A.; Pfaum, J.; Hirschmann, S.; Zhuang, W.; Jaiser, F.; Asawapirom, U.; Rabe, J. P.; Scherf, U.; Neher, D. *Adv. Funct. Mater.* **2004**, *14*, 757.

(10) Chambers, D. K.; Karanam, S.; Qi, D.; Selmic, S.; Losovyj, Y. B.; Rosa, L. G.; Dowben, P. A. *Appl. Phys. A* **2005**, *80*, 483−488.

(11) Themans, B.; Salaneck, W. R.; Bredas, J. L. *Synth. Met*. **1989**, *28*, C359.

(12) Sirringhaus, H.; Brown, P. J.; Friend, R. H.; Nielsen, M. M.; Bechgaard, K.; Langeveld-Voss, B. M. W.; Splering, A. J. H.; Janssen, R. A. J.; Meijer, E. W.; Herwig, P.; De Leeuw, D. M. *Nature* **1999**, *401*, 685.

(13) Rosa, L. G.; Losovyj, Y. B.; Choi, J.; Dowben, P. A. *J. Phys. Chem. B* **2005**, *109*, 7817−7820.

(14) Dowben, P. A.; LaGraffe, D.; Onellion, M. *J. Phys.: Condens. Matter* **1989**, *1*, 6571.

(15) Dowben, P. A.; Choi, J.; Morikawa, E.; Xu, B. The Band Structure and Orientation of Molecular Adsorbates on Surfaces by Angle-Resolved Electron Spectroscopies. In *Handbook of Thin Films, vol. 2, Characterization and Spectroscopy of Thin Film*; 2002; Chapter 2, pp 61−114.

(16) Steinrück, H.-P. *J. Phys.: Condens. Matter* **1996**, *8*, 6465−6509. Plummer, E. W.; Eberhardt, W. *Adv. Chem. Phys.* **1982**, *49*, 533.

(17) McIlroy, D. N.; Zhang, J.; Dowben, P. A.; Heskett, D. *Mater. Sci. Eng., A* **1996**, *217*/*218*, 64−68.

(18) McIlroy, D. N.; Waldfried, C.; McAvoy, T.; Choi, J.; Dowben, P. A.; Heskett, D. *Chem. Phys. Lett.* **1997**, *264*, 168−173.

(19) Stewart, J. J. P. *J. Comput. Chem*. **1989**, *10*, 209.

(20) Stewart, J. J. P. *J. Comput. Chem*. **1989**, *10*, 221.

(21) Caruso, A. N.; Bernard, L.; Xu, B.; Dowben, P. A. *J. Phys. Chem. B* **2003**, *107*, 9620.

(22) Duan, C.-G.; Mei, W. N.; Hardy, J. R.; Ducharme, S.; Choi, J.; Dowben, P. A. *Europhys. Lett.* **2003**, *61*, 81.

(23) Caruso, A. N.; Rajesh, R.; Gallup, G.; Redepenning, J.; Dowben, P. A. *J. Phys. Chem. B* **2004**, *108*, 6910.

(24) Caruso, A. N.; Rajesekaran, R.; Gallup, G.; Redepenning, J.; Dowben, P. A. *J. Phys.: Condens. Matter* **2004**, *16*, 845.

(25) Hill, I. G.; Kahn, A.; Cornil, J.; Santos, D. A. dos; Brédas, J. L. *Chem. Phys. Lett.* **2000**, *317*, 444.

(26) Brown, P. J.; Thomas, D. S.; Khler, A.; Wilson, J. S.; Kim, J.-S.; Ramsdale, C. M.; Sirringhaus, H.; Friend, R. H. *Phys. Rev. B* **2003**, *67*, 064203.

(27) Brown, P. J.; Sirringhaus, H.; Harrison, M.; Shkunov, M.; Friend, R. H. *Phys. Rev. B* **2000**, *63*, 125204.

(28) Apperloo, J. J.; Janssen, R. A. J.; Nielsen, M. M.; Bechgaard, K. *Adv. Mater.* **2000**, *12*, 1594.

(29) Sohn, Y.; Richter, J.; Ament, J.; Stuckless, J. T. *Appl. Phys. Lett.* **2004**, *84*, 76−78.

(30) Ziemelis, K. E.; Hussain, A. T.; Bradley, D. D. C.; Friend, R. H.; Rhe, J.; Wegner, G. *Phys. Rev. Lett.* **1991**, *66*, 2231.

(31) Wohlgenannt, M.; Jiang, X. M.; Vardeny, Z. V. *Phys. Rev. B* **2004**, *69*, 241204R.

(32) Lgdlund, M.; Lazzaroni, R.; Stafström, S.; Salaneck, W. R.; Bredas, J.-L. *Phys. Rev. Lett.* **1989**, *63*, 1841.

(33) Keane, M. P.; Svensson, S.; Brito, A. N. D.; Correia, N.; Lunell, S.; Sjögren, B.; Inganäs, O.; Salaneck, W. R. *J. Chem. Phys.* **1990**, *93*, 6357.

(34) Rhe, J.; Colaneri, N. F.; Bradley, D. D. C.; Friend, R. H.; Wegner, G. *J. Phys.: Condens. Matter* **1990**, *2*, 5465.

(35) Ortega, J. E.; Himpsel, F. J.; Li, D.; Dowben, P. A. *Solid State Commun.* **1994**, *91*, 807.